A 3 Dimensional-Acoustic Current Meter, (3D-ACM)

Mr. Alan J. Fougere
President
Falmouth Scientific, Inc.

Neil Brown
Senior Scientist
Falmouth Scientific, Inc.

Dr. Andrew Kun
Senior Development Engineer
Falmouth Scientific, Inc.

Much has been learned about ocean dynamics by making measurements of ocean currents with traditional electromechanical type current meters. However, flow distortion, large sample volumes, and impeller stalling has limited the ability to use these instruments to make surface and wave deep ocean current measurements. New acoustic measurement techniques offer the potential to overcome these limitations. Here, we present results of laboratory and field tests of a new, low power, acoustic phase shift current meter that transmits a 1 MHz acoustic signal along four paths and uses the along the path phase-shift measurement to resolve the three components of velocity. This technique overcomes the inertial limitations of electromechanical sensors, allowing for the accurate measurement of the small currents expected in the deep ocean, in addition to a small sample volume. Laboratory measurements are presented from tow tank and flume testing. Inter-comparisons of field data from a 4 month long deployment on the ALTOMOOR mooring 90 km southeast of Bermuda, are made with an RD Instruments Broad Band Doppler Profiler, and a UCSB Ocean Physics Laboratory VMCM. Data from a direct inter-comparison of the 3D-ACM with two signal point Doppler type current meters are made (data courtesy of NOAA PMEL). A non-comparative but unique data set from the WHOI Moored Profiler is also examined.

Current meters in routine use today have relatively large, expensive electronics and battery packages and have limited operational life. Current meters using mechanical sensors (rotors or impellers) are vulnerable to damage and are easily stalled by marine fouling or flotsam of various kinds. Existing acoustic current meters using two orthogonal pairs of transducers and an acoustic mirror have poor vertical and horizontal cosine response due to flow interaction with the mirror and the struts used to carry the mooring tension around the pressure housing. These instruments also consume excessive power and hence have limited operational life. A new range of single point Doppler type current meters have also recently been introduced. Due to limited signal to noise, low frequency response, and poor flow directional sensitivity, these units have not demonstrated advantage of very high signal to noise high resolution techniques of direct acoustic phase shift velocity measurement as described by Brown' 92 [1].

A review of the technology employed in the 3D-ACM is in order. The continuous wave type sensors described by Brown [2] are fully implemented in the 3D-ACM. Figure 1 illustrates a Coastal Version of the 3D-ACM acoustic current sensor. The current meter has four acoustic paths. Each acoustic path is 13 cm in length and has a vertical separation of 10.5 cm. It can be shown that only one of the four paths will be significantly contaminated by the wake from the center support strut. The 80528 (Intel 8051 core) microprocessor is used to determine which axis is contaminated by flow interaction with the center support strut and will reject the data from this axis. This is done by simply determining from which quadrant, in the X-Y plane, the current is flowing. Only three axes are required for a complete solution of the X, Y and Z components of velocity, thus permitting the accurate determination of current flow essentially uncontaminated by flow interaction with the center strut.

The photographs shown in figure 2 show the internal details of the production instrument. The design includes a "no moving parts" direction sensor described below. It avoids the need for expensive and fragile gimbals and oil filled damping chambers used in the earlier instruments. The design uses a combination of a very low power, 3 axis magnetometer and 2 axis accelerometer. The data from these sensors are processed in the microprocessor to determine tilt and magnetic direction, and are combined with velocity sensor outputs to determine the N/S and E/W components for vector averaging.

VELOCITY MEASUREMENT:

The new design transmits a 1 MHz continuous wave signal for a period of 2 ms, first in one direction where the total phase shift including the receiver phase shift is measured, and then in the opposite direction where the total phase shift is measured again, using the same receiver. The current velocity is proportional to the difference in phase for the two directions. A simple but accurate, very low power circuit for measuring phase shift at the carrier frequency is used. Since the same receiver is used for both directions, the errors due to the different phase shift of two receivers or offset errors in the phase sensitive detector are eliminated when the difference is taken.

Figure 2

The theory of operation is as follows. If we consider an acoustic path with two transducers at points A and B, where each transducer is alternately transmitting and receiving, we can say that total phase shift between the received and transmitted signals is as follows.

$\Theta_{ab} = \Theta_{ta} + \Theta_{ttab} + \Theta_{rec}$
$\Theta_{ba} = \Theta_{tb} + \Theta_{ttba} + \Theta_{rec}$

Where Θ_{ta} and Θ_{tb} are the phase angles between the applied voltage and the resulting acoustic pressure wave for transducers A and B acting as transmitters. Similarly Θ_{ra} and Θ_{rb} are the phase angles between the output voltage and the arriving acoustic pressure wave for transducers A and B acting as receivers. Θ_{ttab} and Θ_{ttba} are the phase shifts due to the acoustic travel times from A $\rightarrow$ B and from B $\rightarrow$ A respectively. Θ_{rec} is the phase shift through the receiver. It can be shown that for any piezo-electric transducer driven by an essentially zero impedance generator or leaded by an essentially zero impedance receiver, the transmitting and receiving phase angles between the electrical current and the acoustic pressure wave are identical.

$$\therefore \quad \Theta_{ta} = \Theta_{ra}$$

$$\Theta_{tb} = \Theta_{rb}$$

$$\therefore \quad \Theta_{ab} - \Theta_{ba} = \Theta_{ttab} - \Theta_{ttba} \qquad (1)$$

$$= \frac{\omega d}{c - v} - \frac{\omega d}{c + v}$$

Where ω= Angular frequency (rads per sec)
d = Distance between transducers A and B (cm)
c = Velocity of sound (cm per sec)
v = Component of velocity along path A $\rightarrow$ B

$$\therefore \quad \Theta_{ab} - \Theta_{ba} = \frac{2\omega vd}{c^2 + v^2}$$

$$\therefore \quad v = c2 \left[\frac{\Theta_{ab} - \Theta_{ba}}{2\omega d}\right] \qquad (c>>>v)$$

CURRENT METER CIRCUIT OPERATION

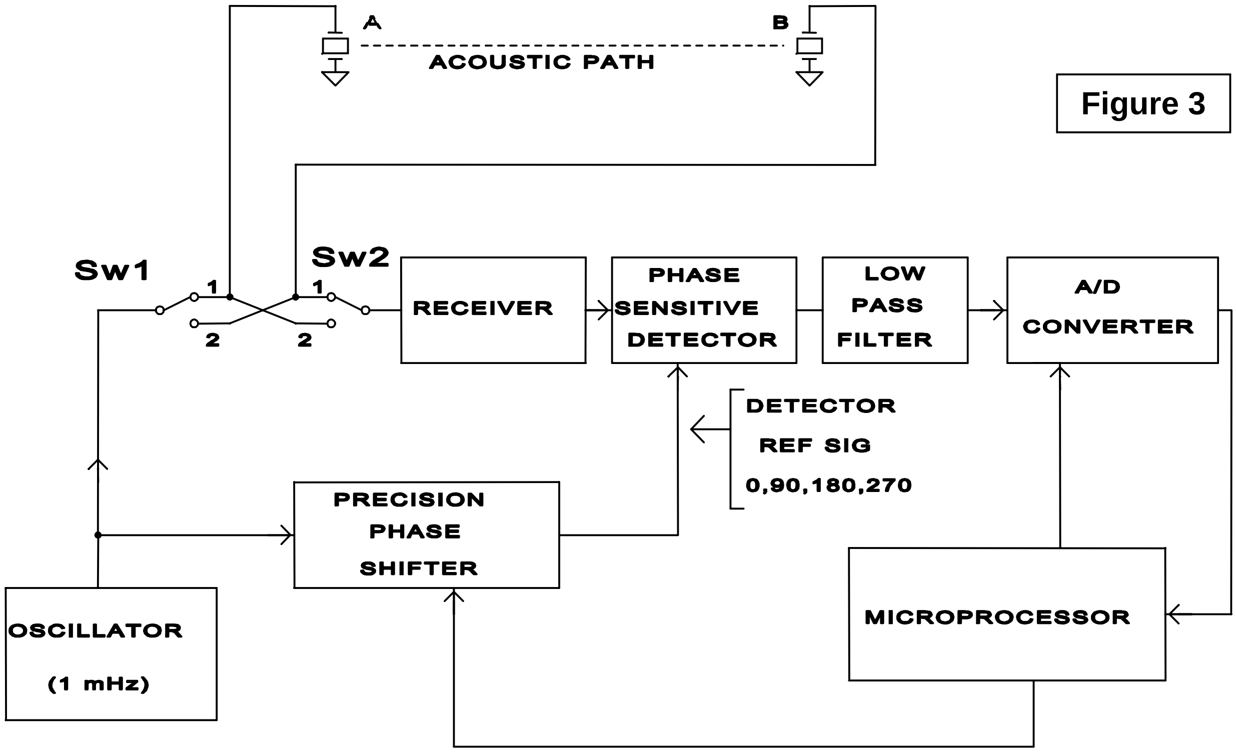

Figure 3 shows a block diagram of the current meter circuit showing just one of the four pairs of transducers and the one set of the switches. The phase shifting circuit output is either 0, 90, 180, or 270 degrees relative the oscillator output, depending on the command from the microprocessor. The circuit operation is as follows:

Firstly the switches Sw1 and Sw2, are set by the processor to connect transducer A to the transmit circuit and transducer B to the receiver thus transmitting from A to B. Initially the phase shifting network is set to 0 degrees and the output of the phase sensitive detector is digitized by the A/D converter and the result is stored.

This is repeated for settings of 90, 180, and 270 degrees. The 0 and 180 degree readings are used to determine the "in-phase component", which is directly proportional to the difference between the 0 and 180 degree readings, regardless of any DC offset in the phase detector. Similarly the 90 and 270 degree readings are used to obtain the "quadrature" component of the received signal. These two signal components are then used to calculate the phase angle between the received signal and the transmitted signal.

The T/R switches, Sw1 and Sw2, are then reversed and the above process is repeated to calculate the phase shift for a signal going from B to A. As shown above, the difference in phase shift for signals going from B to A compared to A to B is then directly proportional to the component of current velocity parallel to the acoustic path between A and B. The above process is then repeated for the remaining 3 acoustic paths and the results are temporarily stored in the micro-processor memory.

For this scheme to work accurately, it is necessary that the impedance of both the transmit and receive circuits be very small, compared with impedance of the transducer. When these conditions are met, the phase angle between the acoustic and electrical signals are the same for each transducer, whether it is transmitting or receiving, thus ensuring the integrity of the phase shift information. Tow testing of the instrument has shown zero errors less than 0.3 cm/sec and that the phase measuring circuit works well and gives stable and linear results. A flume test, figure 4, shows that the unit has very well defined cosine response.

Figure 4

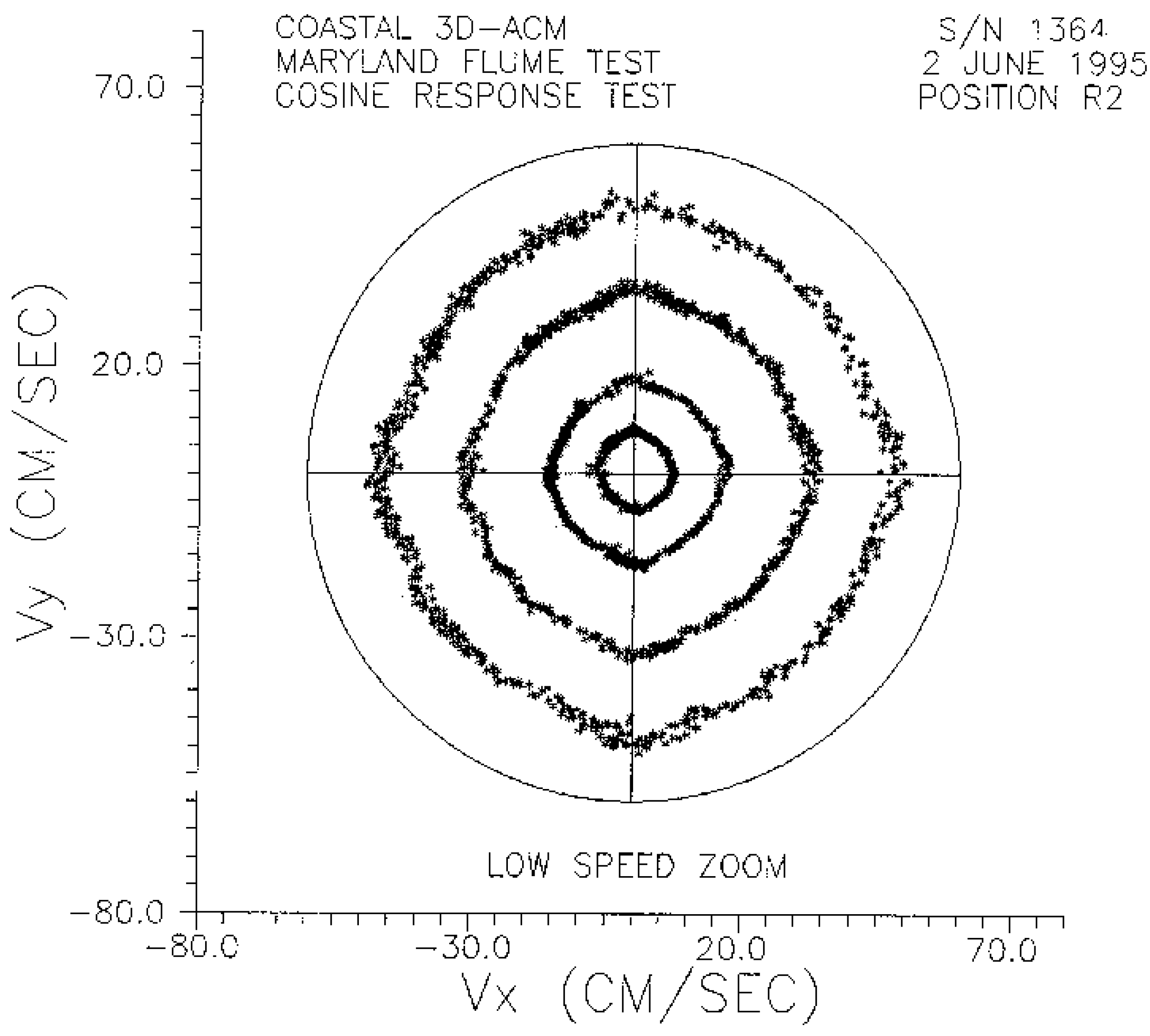

PHASE MEASURING CIRCUIT

The phase sensitive detector shown in figure 3 ideally can be treated as an analog multiplier whose output is the instantaneous product of the two inputs.

$$E_s = K_s \; SIN(\varpi\tau + \Theta_s)$$

$$E_r = K_r \; SIN(\varpi\tau + \Theta_r)$$

Where Ks, Kr are constants

$$\therefore \quad E_{out} = E_s \times E_r$$

$$= \frac{K_s K_r}{2} [\cos(\Theta_s - \Theta_r) - (2\varpi\tau + \Theta_r)]$$

Low pass filtering E_{out} gives E_{dc}

$$\therefore \quad E_{dc} = K \cos(\Theta_s - \Theta_r) + E_{os}$$

Where $K = \frac{K_s K_r}{2}$

and E_{os} = Zero offset of the detector

If $\Theta_r = 0$, then $E_0 = E_{dc} = K \cos(\Theta_s) + E_{os}$

If $\Theta_r = 90$, then $E_{90} = E_{dc} = -K \cos(\Theta_s) + E_{os}$

If $\Theta_r = 180$, then $E_{180} = E_{dc} = -K \cos(\Theta_s) + E_{os}$

If $\Theta_r = 270$, then $E_{270} = E_{dc} = K \cos(\Theta_s) + E_{os}$

$$E_0 - E_{180} = 2K \cos(\Theta_s)$$

$$E_{270} - E_{90} = 2K \sin(\Theta_s)$$

$$\Theta_s = \arctan\left[\frac{(E270 - E90)}{(E0 - E180)}\right]$$

Hence Θ_s is independent of the gain or any d.c. offsets in the phase sensitive detector. The only requirement is that there be a linear relationship between the detector output and the cosine of the phase angle between the signal and reference input.

DIRECTION SENSOR OPERATION

Figure 5

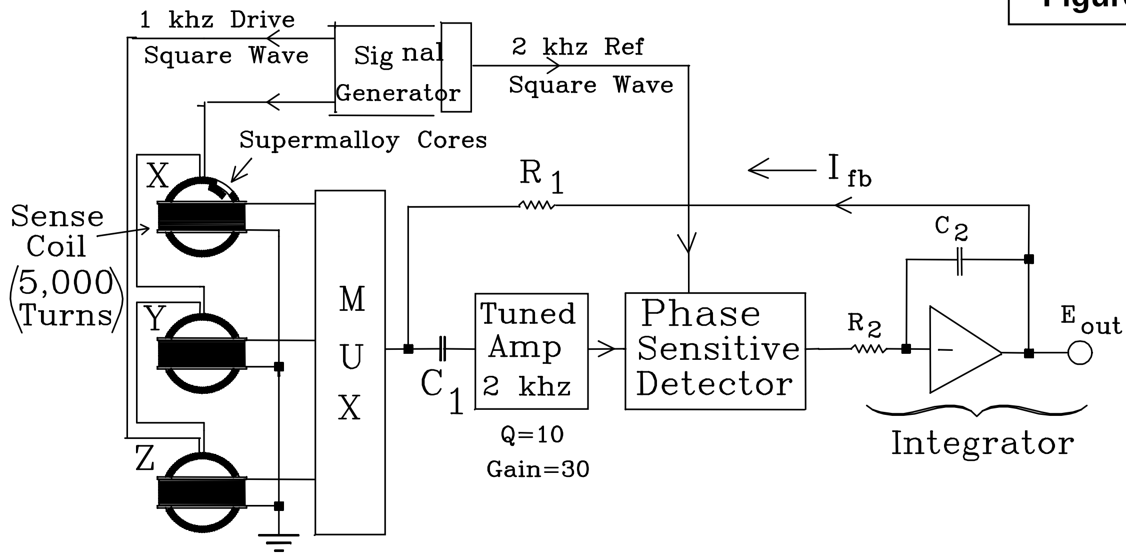

The direction sensor consists of a 3 axis fluxgate magnetometer designed for very low power consumption and an electrolytic type, 2-axis tilt sensor. The flux gate magnetometer achieves very low power consumption by using a magnetic core of very small total volume, thus reducing the energy required to magnetically saturate the core. The X and Y axes of the magnetometer are parallel to the X and Y axes of the tilt sensor. Small errors in alignment of any of the axes of the sensors will be determined at the time of calibration and numerically corrected by the processor. The combined power consumption for the 3 magnetometers and 2 accelerometers is less than 2.4 mw.

Figure 5 is a simplified schematic of the magnetometer. It is an adaptation of the "ring-core" design described by Geyer [3]. Each axis consists a Supermalloy tape wound bobbin core with drive winding on the core and a "sense coil" surrounding the outside of the toroid with its axis parallel to the plane of the core. The drive winding of the 3 cores are connected in series and excited with a 1 KHz square wave of sufficient amplitude to saturate the core. In the absence of any d.c. magnetic field, the signal in each sense coil contains only odd harmonics of the drive signal, because all parts of the core go into saturation at the same instant. However the presence of a d.c. field will cause one side of the core to go into saturation slightly before the other (d.c. and a.c. components add on one side and subtract on the other). This results in an unbalance signal in the sense coil. This unbalance signal results in a 2 KHz component in the output of each sense coil. The 3 sense coils are sequentially connected to the input of an amplifier tuned to 2 KHz. The unbalance signal is amplified in the tuned amplifier (see fig 5) and detected by the phase sensitive detector. Since the detector reference is a 2 KHz square wave the output will contain a d.c. term, which is integrated in the integrator. The d.c. output from the integrator is fed back to the sense coil. The complete circuit is a negative feedback system, which balances the earth's field with an equal and opposite field in the sense coil. The field generated by the sense coil is proportional to the product of the number of turns and the feedback current I_{fb}. To minimize power consumption, the maximum value of required feedback current was minimized by winding the sense coil with a large number of turns. The output voltage E_{out} is given by

$$E_{out} = I_{fb}.R_1$$

Hence E_{out} is directly proportional to the component of magnetic field (H) parallel to the axis of the sense coil. The advantage of this negative feedback scheme is that the calibration of the magnetometer is essentially insensitive to changes in the magnetic properties of the core.

Bermuda Test Inter-comparison August 24 - December 12 1996

In August of 1996, a standard production version of the 3D-ACM was deployed in conjunction with the jointly operate ALTMOOR Test Mooring of the Bermuda Coast [4]. ALTMOOR is an engineering test mooring operated by Woods Hole Oceanographic and The University of California Santa Barbara (UCSB), with principal investigators of Dan Frye and Tom Dickey, respectively.

The ALTMOOR mooring uses a surface deployed 2 meter syntactic foam float located in 5000 meters of water depth. The 3D-ACM was located at approximately 90 meters from the surface and directly below a UCSB Vector Measuring Current Meter, (VMCM), and approximately 50 meters above a RD Instruments Broad Band Acoustic Doppler Profiler (ADCP). Shown in figure 6 are the Zonal, Meridional, and Speed inter-comparisons for the duration of the deployment. In figure 7 the differences for the same data are shown. The data speed correlations for 2 hour averages are shown in figures 8 & 9. The data direction correlations are shown in figures 10 & 11. Finally in figure 12, is a Current Spectra diagram for all three instruments.

Figure 6

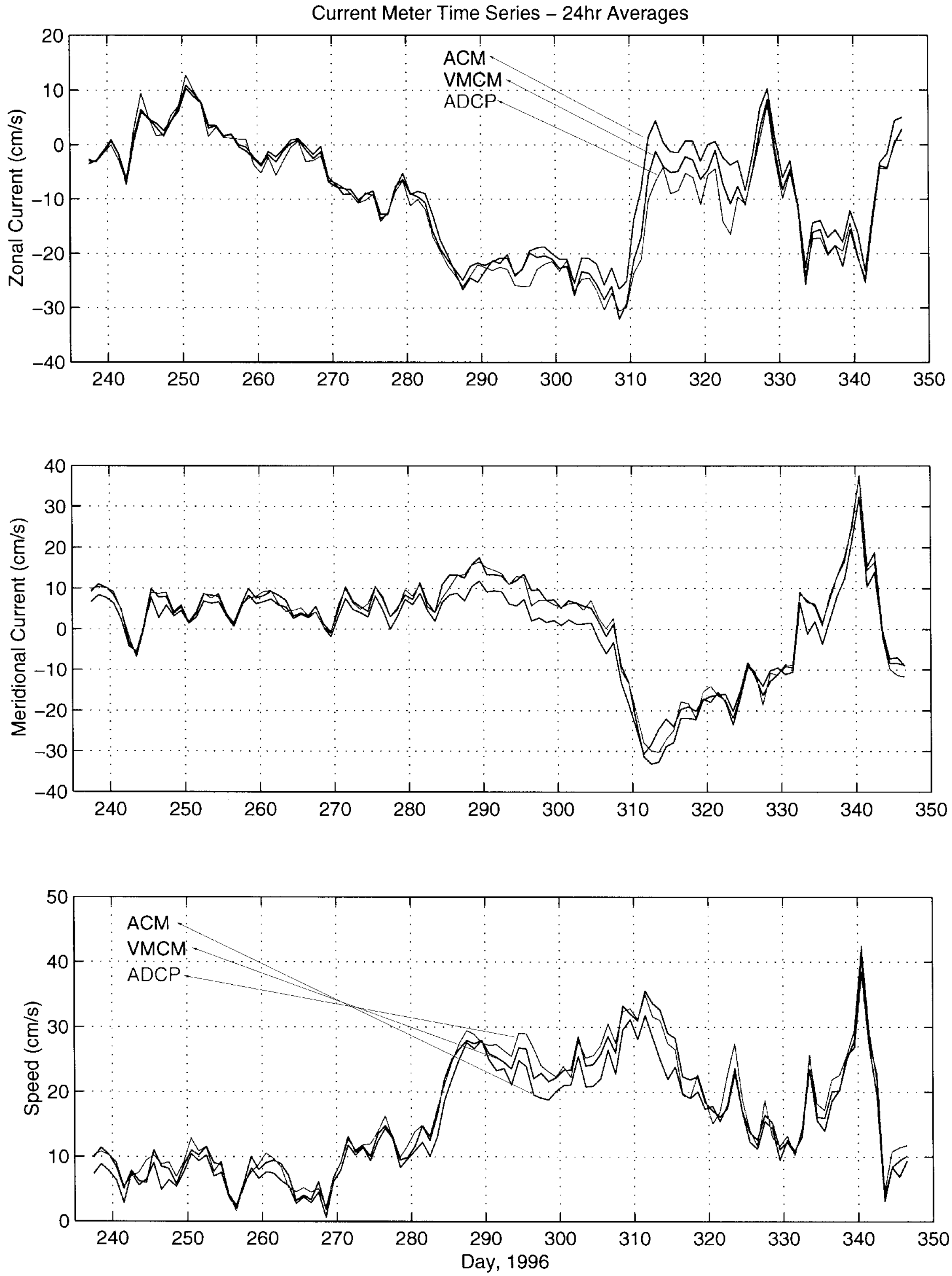
Current Meter Time Series – 24hr Averages
ACM
VMCM
ADCP
Zonal Current (cm/s)
Meridional Current (cm/s)
Speed (cm/s)
Day, 1996

Figure 7

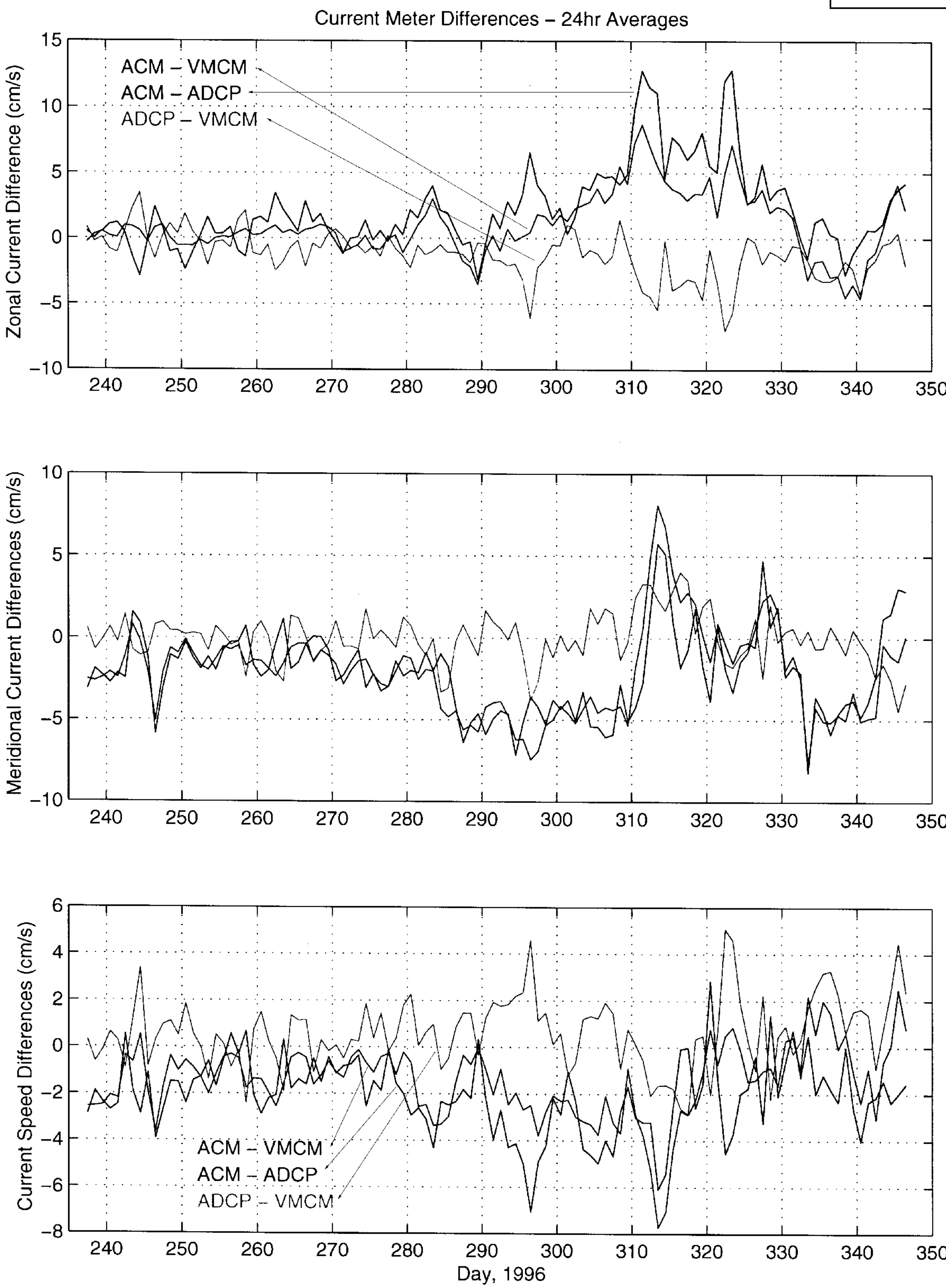
Current Meter Differences – 24hr Averages
ACM – VMCM
ACM – ADCP
ADCP – VMCM
Zonal Current Difference (cm/s)
15
10
5
0
-5
-10
240
250
260
270
280
290
300
310
320
330
340
350
Meridional Current Differences (cm/s)
10
5
0
-5
-10
Current Speed Differences (cm/s)
6
4
2
0
-2
-4
-6
-8
ACM – VMCM
ACM – ADCP
ADCP – VMCM
Day, 1996

Figure 8

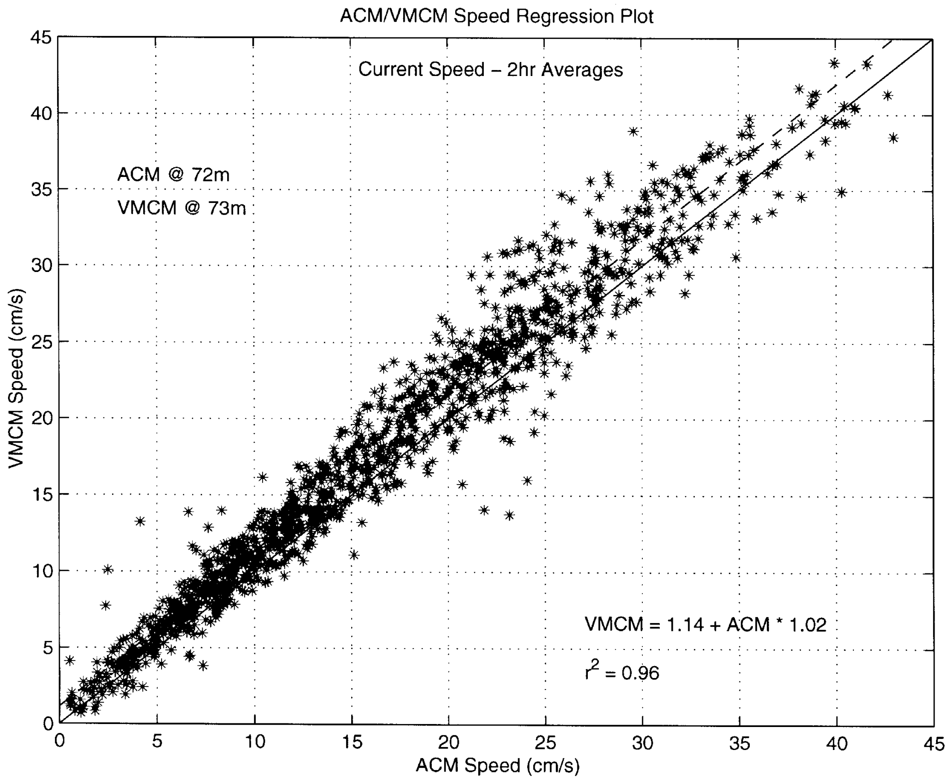

Figure 9

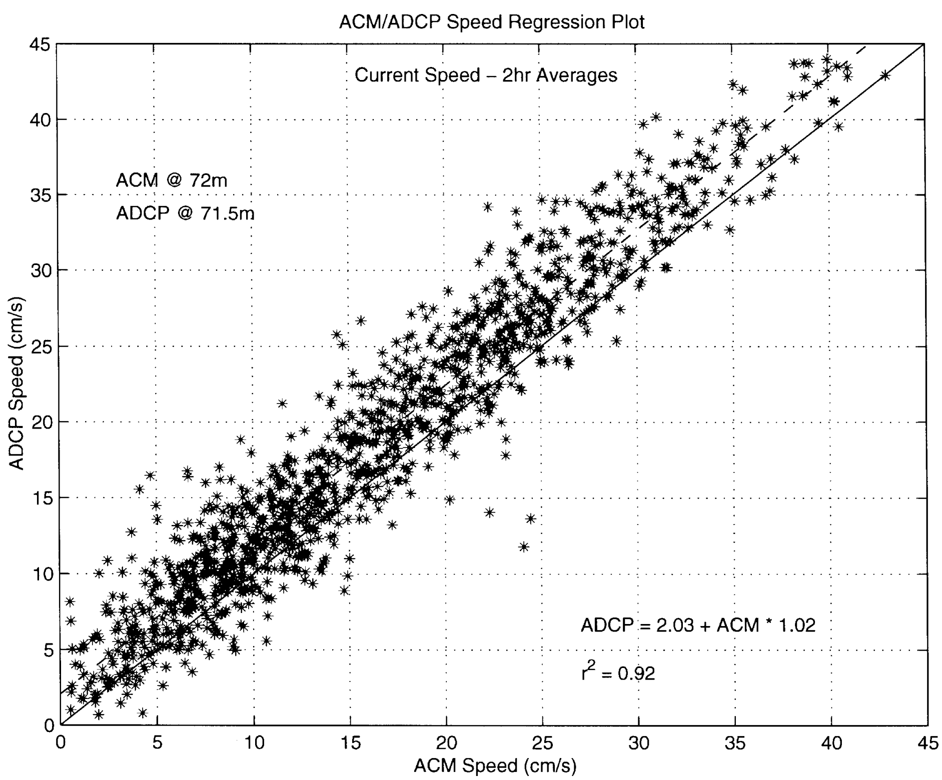

Figure 10

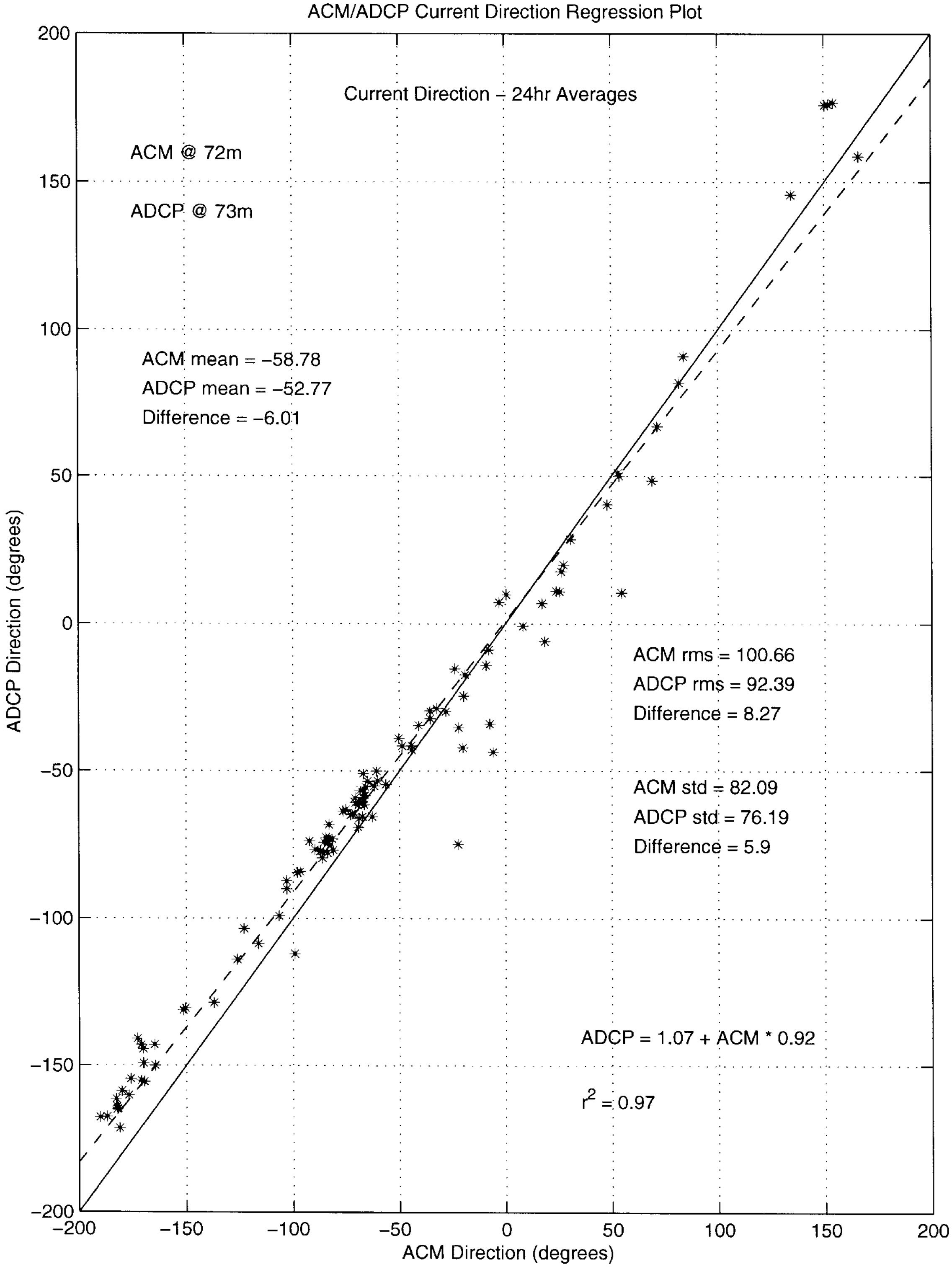
ACM/ADCP Current Direction Regression Plot
Current Direction – 24hr Averages
ACM @ 72m
ADCP @ 73m
ACM mean = −58.78
ADCP mean = −52.77
Difference = −6.01
ACM rms = 100.66
ADCP rms = 92.39
Difference = 8.27
ACM std = 82.09
ADCP std = 76.19
Difference = 5.9
ADCP = 1.07 + ACM * 0.92
r2 = 0.97
ADCP Direction (degrees)
ACM Direction (degrees)
200
150
100
50
0
−50
−100
−150
−200
−200
−150
−100
−50
0
50
100
150
200

Figure 11

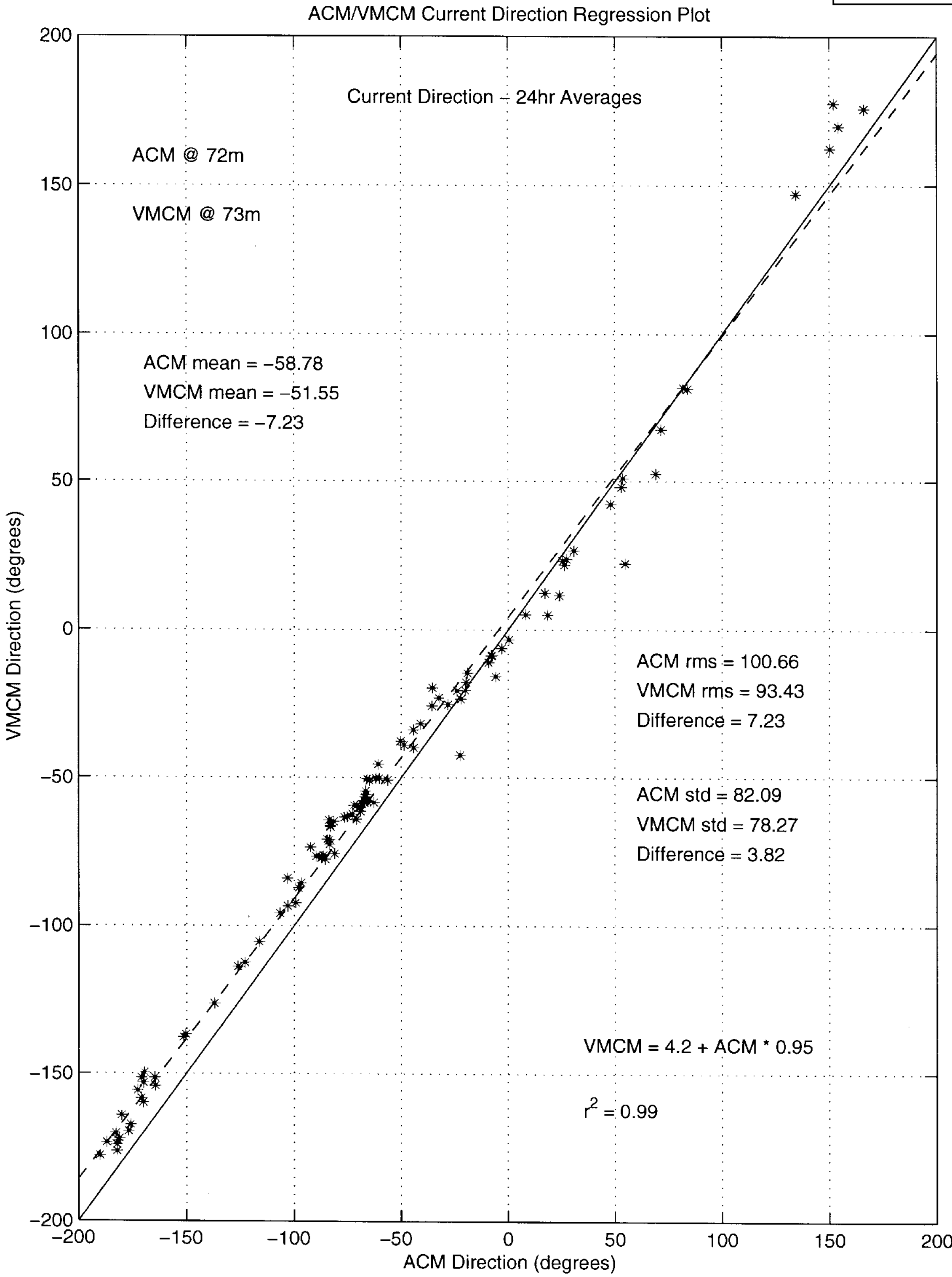
ACM/VMCM Current Direction Regression Plot
Current Direction – 24hr Averages
ACM @ 72m
VMCM @ 73m
ACM mean = −58.78
VMCM mean = −51.55
Difference = −7.23
ACM rms = 100.66
VMCM rms = 93.43
Difference = 7.23
ACM std = 82.09
VMCM std = 78.27
Difference = 3.82
VMCM = 4.2 + ACM * 0.95
r^2 = 0.99
VMCM Direction (degrees)
ACM Direction (degrees)
200
150
100
50
0
−50
−100
−150
−200
−200
−150
−100
−50
0
50
100
150
200

Figure 12

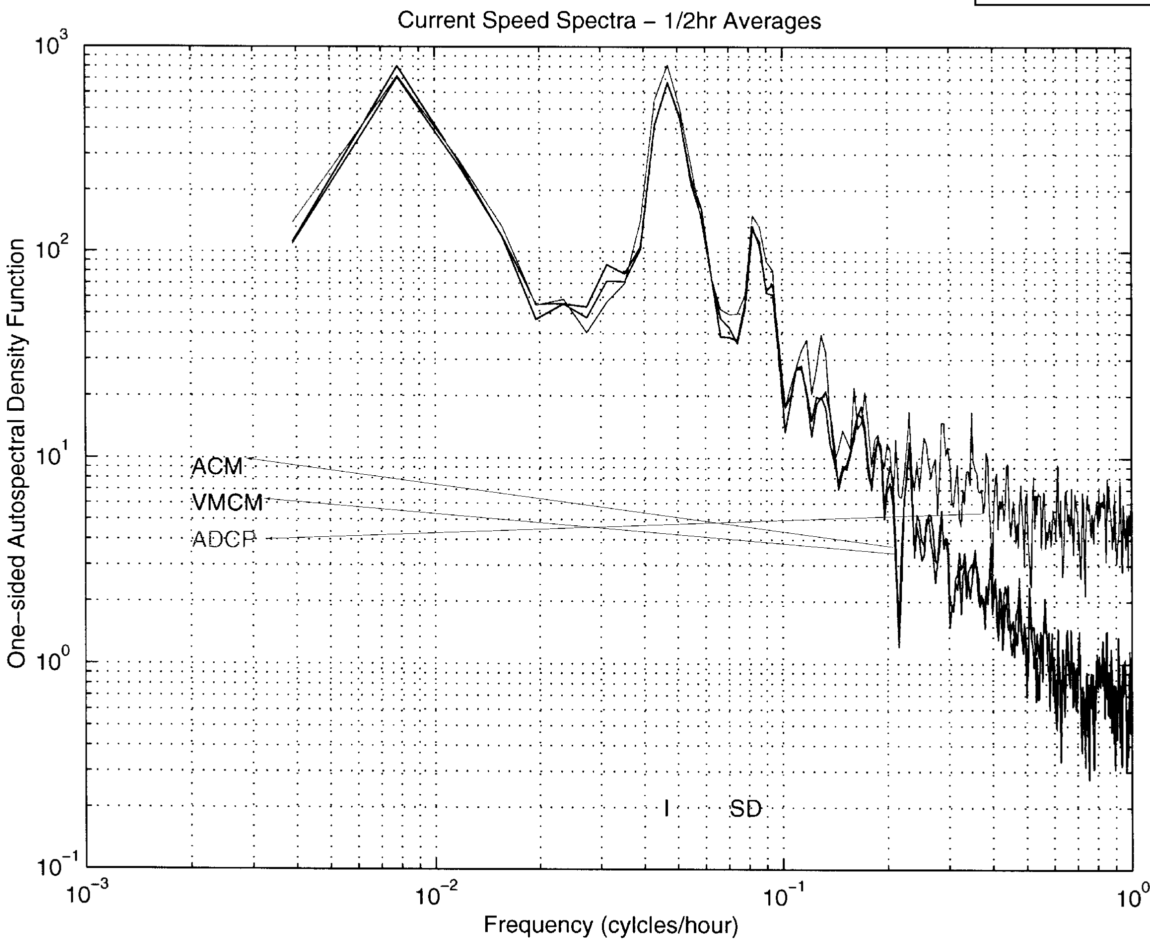

The data presented indicates that even when deployed on a dynamic surface mooring, the 3D-ACM is capable of measurements of the same quality and accuracy as two well established techniques for the measurement of ocean currents. This is the most demanding environment for the measurement of ocean currents where horizontal scales of 0 - 10 cm/sec are being measurement with an instrument which may have vertical velocities of up to 100 cm/sec due to wave action on the surface expression.

NOAA PMEL Inter-comparison Test December-January 1996:

NOAA PMEL performed an inter-comparison of four different current meters in mid winter 1996 [5]. The test was conducted on a subsurface mooring in Puget Sound. The instruments included an FSI Coastal 3D-ACM, two point Doppler current meters, a salvonious rotor, and, an acoustic Doppler profiler used as a reference sensor. The mooring was deployed for 30 days and data analysis and processing was performed by NOAA*.

(* one 3 beam point Doppler data was edited by the manufacturer due data corruption caused by the disturbance of the mooring cable, eliminating all data above 45 cm/sec).

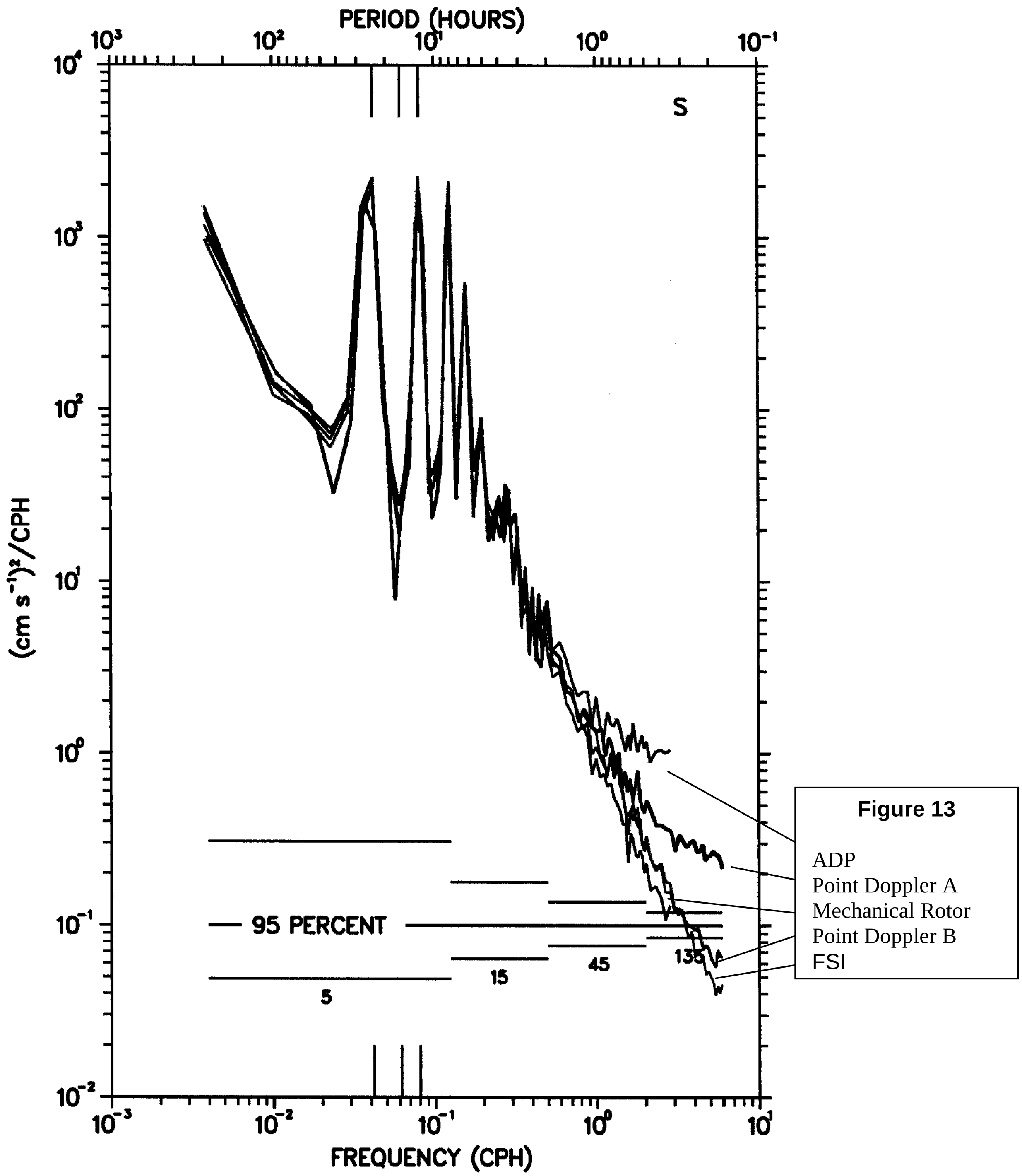

PERIOD (HOURS)
S
95 PERCENT
5
15
45
135
(cm s⁻¹)²/CPH
FREQUENCY (CPH)
Figure 13
ADP
Point Doppler A
Mechanical Rotor
Point Doppler B
FSI

Figure 14

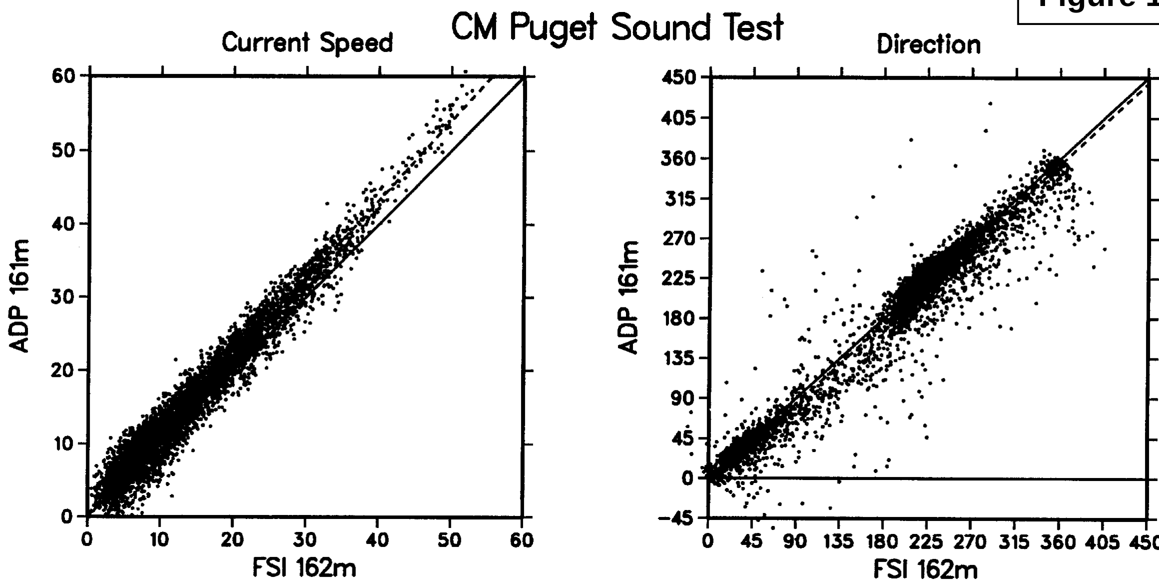

FROM 2200 20 DEC 96 TO 1900 22 JAN 97

	MIN	MAX	MEAN	STD DEV
x:	0.500	52.77	15.33	9.384
y:	0.100	60.63	16.80	10.05

n: 4735 df: 4733 r: 0.98 t: 314.69 (SIGNIFICANT)

y = a + bx: a = 0.348 , b = 1.07 (Orth)

95% c. i. : a = 0.118 , b = 0.656E−2

Difference: RMS = 2.64, Mean = 1.47(0.06)

FROM 2200 20 DEC 96 TO 1900 22 JAN 97

	MIN	MAX	MEAN	STD DEV
x:	−21.70	405.1	178.1	98.34
y:	−69.00	421.6	172.0	98.31

n: 4735 df: 4733 r: 0.97 t: 292.92 (SIGNIFICANT)

y = a + bx: a = −6.12 , b = 1.00 (Orth)

95% c. i. : a = 1.33 , b = 0.656E−2

Difference: RMS = 23.46, Mean = −6.18(0.64)

Shown in figure 13 is a noise spectra plot for the all instruments. It can be seen at the higher wave numbers that the 3D-ACM offers significant performance over Doppler type measurements, and has, comparable noise to rotors which actually average out high frequency noise due to mechanical momentum of the sensor. Shown in figure 14 is a comparison plot of the performance of the FSI to the ADP. Data had not been corrected for sound velocity and shows a strong speed and directional correlation to the reference unit. As a result of this test the sensitivity factor for the 3D-ACM has been changed from unity to 1.07 to correct of the slight reduction in path length due to the acoustic fingers.

NEW DEVELOPMENTS

FSI working in conjunction with Dr. Steve Anderson of WHOI has identified the electronic compass as the largest single source of errors in the measurement of ocean currents. The compass is often effected by inaccuracies in the determination of the gravity vector (tilt) which also effects the geometric translations of instrument velocities to earth reference velocities. The compass is also effected by local magnetic disturbances caused by the instrument, its required components, housing, battery, etc. FSI has developed unique computer controlled Hemholtz calibration facilities to allow for precision calibration of magnetic sensors. New instruments have been improved with the incorporation of "spin" calibration algorithms to eliminate "hard iron" magnetic effects. Hard Iron effects being described as correction of magnetic effects, which rotate with the instrument, such as batteries, housings, mooring frames. However, we continue to believe that dramatic improvement can be made by the introduction of one of several new technologies to the very low power measurement of instrument heading & tilt. We included in these new techniques magnetoresistive materials whose electrical properties vary when subjected to DC magnetic fields. We are also introducing micro-machined semi conductor accelerometers for the measurement of the tilt angle reducing the errors associated with electrolytic fluid type tilt sensors. FSI expects to introduce and improve compass utilize micro-machined tilt sensors in the later half of 1998.

We have also recently introduced a Wave version of the 3D-ACM. This unit combines our low noise high frequency velocity measurement with Silicon machined *0.01%* F.S. precision pressure sensor for the measurement of wave height, tides, and waver directional spectra. This unit has a 6 hertz data rate and is capable of performing the wave spectra calculation's on-board allowing for direct telemetry to shore stations. This instrument was described by Dr Kun [6]. The new instrument allows the user to measure surface wave amplitude and direction, along with tide and tidal flow, from a single subsurface instrument. If the single instrument is combined with three additional "synchronized" pressure sensors, a complete six-wire-equivalent wave measurement can be attained.

MOORED PROFILER 3D-ACM:

A specially configured 3D-ACM has been fabricated and successfully deployed on the Woods Hole Oceanographic Moored Profiler [7]. The Moored Profiler, is essentially a sensor platform that cycles vertically along a conventional, plastic-jacketed mooring wire while acquiring repeated, fine-scale profiles of ocean water properties and current. It consists of a propulsion system, controller with data logger, sensor suite, battery pack and buoyancy elements, all contained within a streamlined oblate-spheroidal housing 80 cm x 40 cm in dimension. A traction drive system propels the instrument along a length of conventional plastic-jacketed wire rope in a subsurface oceanographic mooring at speeds of ~30 cm s^{-1}, and repeatedly traverses that length based on a user defined operation program. Maximum design depth is 5000 m, and design endurance is one million meters (200 vertical profiles of 5000 m).

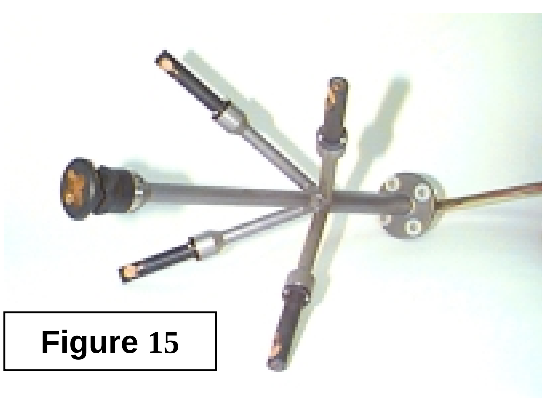

Figure 15

The 3D-ACM was configured to allow for very high accuracy horizontal current measurements from this vehicle system. The Moored Profiler application, the 3D-ACM is equipped with a modified, remote sensor head allowing the electronics to be mounted within the streamlined fairing, figure 15. The most dramatic change to the instrument is the re-orientation of the instrument's four acoustic velocity measurement paths into a 45-degree pyramid configuration. This geometry provides two orthogonal paths in the horizontal plane and two in the vertical plane. When profiling, because the instrument is free to align with the incident horizontal flow, three acoustic paths are always upstream of wakes from the support struts and return valid current data. These three are used during post processing to deduce the three components of flow relative to the Profiler. This allows for time series measurements to be made using a single instrument making daily profiles. The vehicle system was developed by Dr. John Toole (WHOI). The data set is from a recent deployment of the system off the US eastern continental shelf. The unit demonstrates the ability of the electronics to utilize a remote sensor head with no degradation in the performance of the velocity measurement. As the is optimized for profiling it affords the user a data set coves 1500 meters of water depth with resolution and precision not possible using conventional ADCPs.

In figure 16 data from a recent trial made on the U.S. continental slope. In this deployment the instrument was programmed to profile continuously in time for the 37-day test deployment, 501 profiles were obtained [8]. Baroclinic eddies passed the mooring site on two occasions, causing isotherms and isohalines to dip by 100 m or more. These features can be seen in the observed current data, superimposed on the prevailing flow to the northwest during this test deployment.

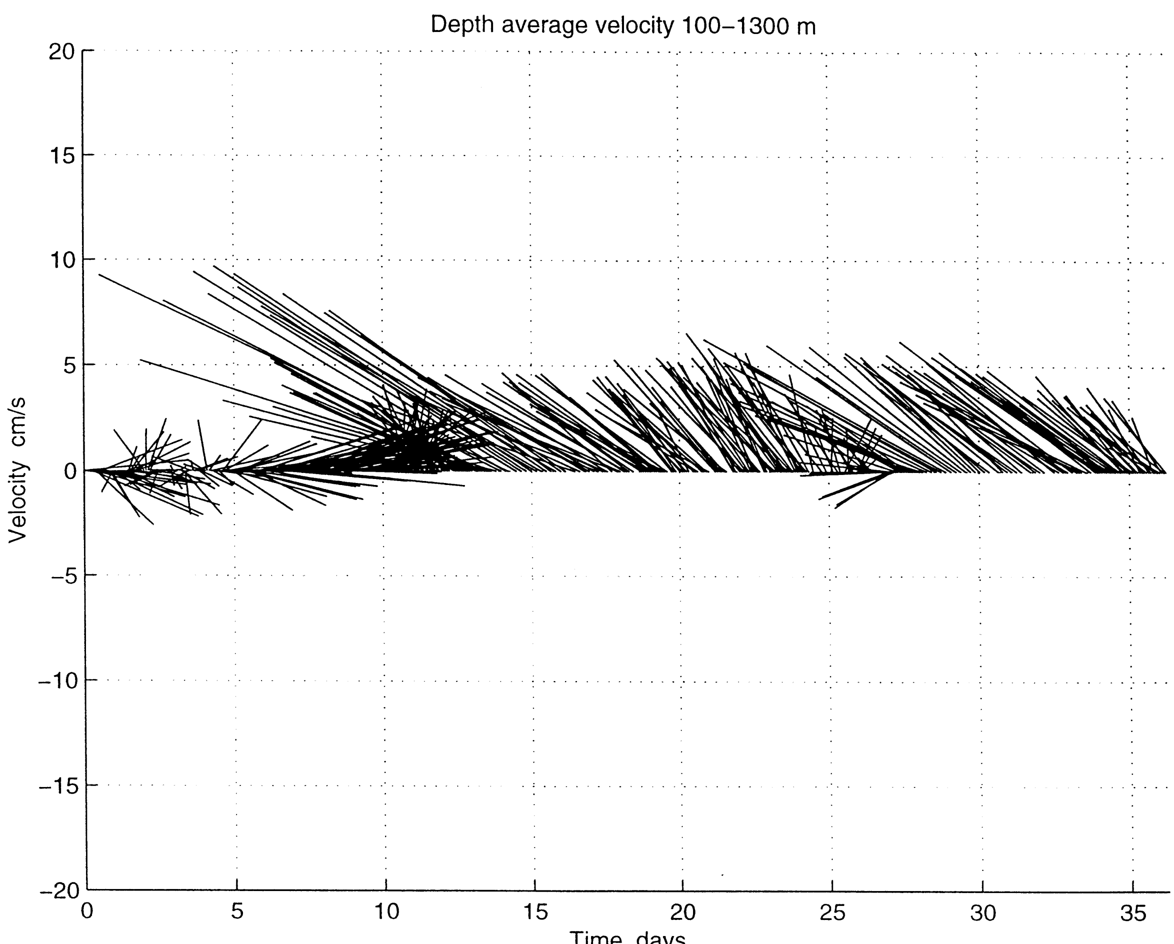

Figure 16

CONCLUSION:

The 3D-ACM demonstrated its ability to return high quality oceanographic current data, which compares well with other traditional technologies. FSI continues to expand the product offerings of this new technology including custom adaptations to address specific sampling requirements such as the Moored Profiler, Wave Height and Direction Measurement.

REFERENCES:

[1] Brown, N.L. A Simple Low Cost Acoustic Current Meter, Oceanology International, 10-13 March 1992.

[2]Gytre, Trygve "Ultrasonic Measurements of Ocean Currents Down to 1 mm/sec" IERE Conf. Proc. #32 Instrumentation in Oceanography, 23 -25 Sept., University College N. Wales, Bangor, U.K., pp 69-80.

[3] Geyger, W.A., "The Ring-Core Magnetometer – A New Type of Second Harmonic Fluxgate Magnetometer", Trans. AIEE (Commun. Electron.), vol. 81, pp. 65-73, Mar. 1962.

[4] Andrew L. K. and Fougere, A. J., "New Wave Direction and Spectrum Measurement Technique", The Third International Symposium on Ocean Wave Measurement and Analysis, November 3-7, 1997, Virginia Beach, Virginia.

[5] Gilboy, Tim, Dickey, T., "Intercomparison Results of Current Measurements From an ADCP, a VMCM, and a New Falmouth Scientific, Inc. 3D Acoustic Current Meter at the Bermuda Testbed Mooring Site", Presented February 1998, American Geophysical Union, Ocean Sciences Meeting, San Diego, CA.

[6] Freitag, Paul, " Puget Sound Current Meter Test Mooring", PMEL/NOAA Internal Report , February 1997. (Please note permission to use this data has not been given, resulting in the elimination of specific identification of manufacturers form the data set.)

[7] Frye, D.E., K.W. Doherty, A.A. Hinton, and J.M. Toole. A moored, profiling instrument for long-term hydrographic observations. EOS, 76 no. 3 suppl. pg OS77, 1996.

[8] Fougere, A.J., and Toole, J. "Physical Oceanographic Time-Series Sensors", Sea Technology, ST Applications Feature, February 1998 Issue.